IEEE Photonics Journal
An IEEE Photonics Society Publication

Open Access

100 Gb/s Multicarrier THz Wireless Transmission System With High Frequency Stability Based on A Gain-Switched Laser Comb Source

Volume 7, Number 3, June 2015

H. Shams, Member, IEEE
T. Shao
M. J. Fice, Member, IEEE
P. M. Anandarajah, Senior Member, IEEE
C. C. Renaud, Member, IEEE
F. Van Dijk, Member, IEEE
Liam P. Barry, Fellow, IEEE
Alwyn J. Seeds, Fellow, IEEE

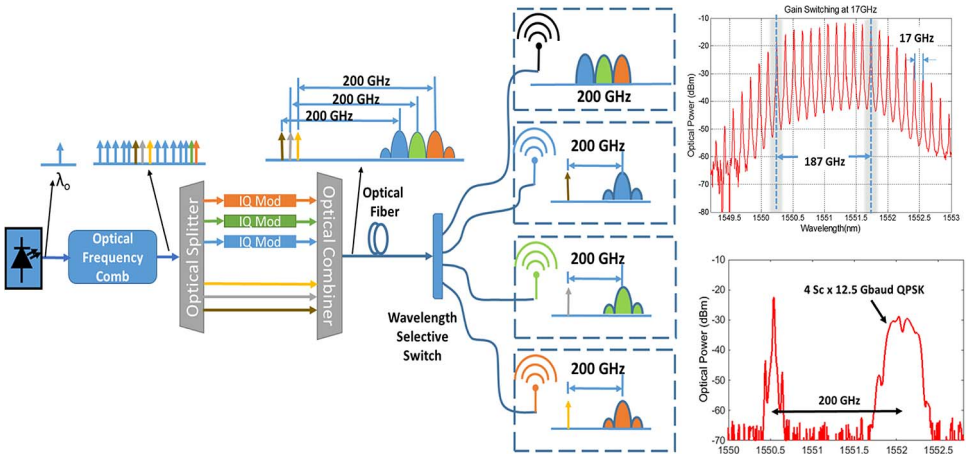

DOI: 10.1109/JPHOT.2015.2438437
1943-0655 © 2015 IEEE

IEEE photonics SOCIETY

IEEE

100 Gb/s Multicarrier THz Wireless Transmission System With High Frequency Stability Based on A Gain-Switched Laser Comb Source

H. Shams,[1] *Member, IEEE*, T. Shao,[2] M. J. Fice,[1] *Member, IEEE*, P. M. Anandarajah,[2] *Senior Member, IEEE*, C. C. Renaud,[1] *Member, IEEE*, F. Van Dijk,[3] *Member, IEEE*, Liam P. Barry,[2] *Fellow, IEEE*, and Alwyn J. Seeds,[1] *Fellow, IEEE*

[1]Department of Electronic and Electrical Engineering, University College London, London WC1E 7JE, U.K.
[2]Radio and Optical Communications Laboratory, Rince Institute, Dublin City University, Dublin, Ireland
[3]III-V Lab, 91767 Palaiseau, France

DOI: 10.1109/JPHOT.2015.2438437

Manuscript received April 29, 2015; revised May 21, 2015; accepted May 21, 2015. Date of publication June 1, 2015; date of current version June 12, 2015. This work was supported in part by the Engineering and Physical Sciences Research Council programme grant Coherent Terahertz Systems (COTS) (EP/J017671/1), by the European Commission through the European project iPHOS (Grant Agreement 257539), and by Science Foundation Ireland through the CTVR programme (10/CE/I1853). Corresponding author: H. Shams (e-mail: h.shams@ucl.ac.uk).

Abstract: We propose and experimentally demonstrate a photonic multichannel terahertz (THz) wireless system with up to four optical subcarriers and total capacity as high as 100 Gb/s by employing an externally injected gain-switched laser comb source. Highly coherent multiple optical carriers with different spacing are produced using the gain switching technique. Single- and multichannel Terahertz (THz) wireless signals are generated using heterodyne mixing of modulated single or multiple carriers with one unmodulated optical tone spaced by about 200 GHz. The frequency stability and the phase noise of the gain switched comb laser are evaluated against free-running lasers. Wireless transmission is demonstrated for single and three optical subcarriers modulated with 8 or 10 GBd quadrature phase-shift keying (QPSK) (48 or 60 Gb/s, respectively) or for four optical subcarriers modulated with 12.5 GBd QPSK (100 Gb/s). The system performance was evaluated for single- and multicarrier wireless THz transmissions at around 200 GHz, with and without 40 km fiber transmission. The system is also modeled to study the effect of the cross talk between neighboring subcarriers for correlated and decorrelated data. This system reduces digital signal processing requirements due to the high-frequency stability of the gain-switched comb source, increases the overall transmission rate, and relaxes the optoelectronic bandwidth requirements.

Index Terms: Microwave photonics, radio-over-fiber, fiber optics and optical communications.

1. Introduction

High-speed Terahertz (THz) wireless communications have attracted great interest for short-distance ultrahigh data rate mobile applications [1]. Several systems have been demonstrated

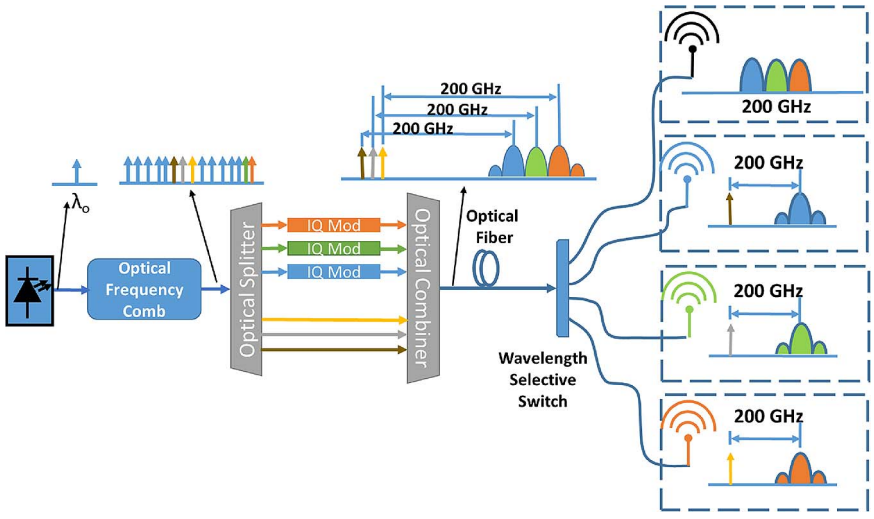

Fig. 1. Block diagram of photonic multichannel THz system for frequency reuse.

based on heterodyne detection for increasing the bit rate up to 100 Gbit/s by using spectrally efficient modulation formats and polarization division multiplexing (PDM) systems [2]. A multi-carrier-based system with optical subcarriers was demonstrated in the W-band to maximize the overall channel data rate and to achieve high spectral efficiency [3]. The wireless transmission window in the 200 GHz band is of strong interest due to low atmospheric transmission losses. Data rates of up to 100 Gbit/s were achieved at 237.5 GHz by using different modulation formats for each channel and a monolithic millimeter-wave integrated circuit (MMIC) receiver [4]. Recently, we demonstrated 75 Gbit/s multichannel transmission at 200 GHz carrier frequency using two free running lasers and a digital coherent receiver [5]. However, the frequency spacing between two lasers is not constant and their phases fluctuate continuously. Therefore, carrier recovery and carrier phase noise correction processes are needed in the digital signal processing (DSP) at the receiver, which increase the processing time, complexity, and system power consumption. In addition, the stability of the generated THz signal using this technique may not meet future standards for wireless transmission at frequencies above 100 GHz [6].

In this paper, we demonstrate experimentally photonic generation of multicarrier THz wireless signals at up to 100 Gb/s using an externally injected gain-switched optical comb source. Unlike previous work using two free-running lasers [5], the gain-switched comb produces phase-correlated optical tones with carrier-to-noise ratio (CNR) greater than 40–45 dB [7]. Single- and multi-channel THz wireless signals were generated using heterodyne mixing of the modulated QPSK optical carrier/s with one unmodulated optical tone spaced by about 200 GHz from the modulated tone/s. Wireless transmission was achieved for single and three optical subcarriers modulated with 8 or 10 Gbaud QPSK (48 Gbit/s or 60 Gbit/s, respectively) or for four optical subcarriers modulated with 12.5 Gbaud QPSK to achieve 100 Gbit/s. For the 100 Gb/s, 4 subcarriers configuration, the system performance was evaluated back to back (B2B) and with 40 km of standard single mode fiber (SSMF) between the optical transmitter and the antenna unit (AU). In this system, the use of the gain-switched comb source offers advantages such as reconfigurable frequency selection and frequency offset stability, which reduces the level of DSP processing that is required for demodulation. This arrangement would also be suitable for generating the transmitted channels at the same carrier frequency, allowing a frequency reuse system or different frequency carriers giving it more flexibility, as illustrated in Fig. 1. By using a comb source, a high-spectral-purity THz signal is generated with frequency stability determined by the RF signal driving the gain-switched laser. In addition, the multichannel THz approach increases the overall transmission capacity and reduces the bandwidth requirement for drive electronics and electro-optic devices. The achieved 100 Gbit/s with four channels increased

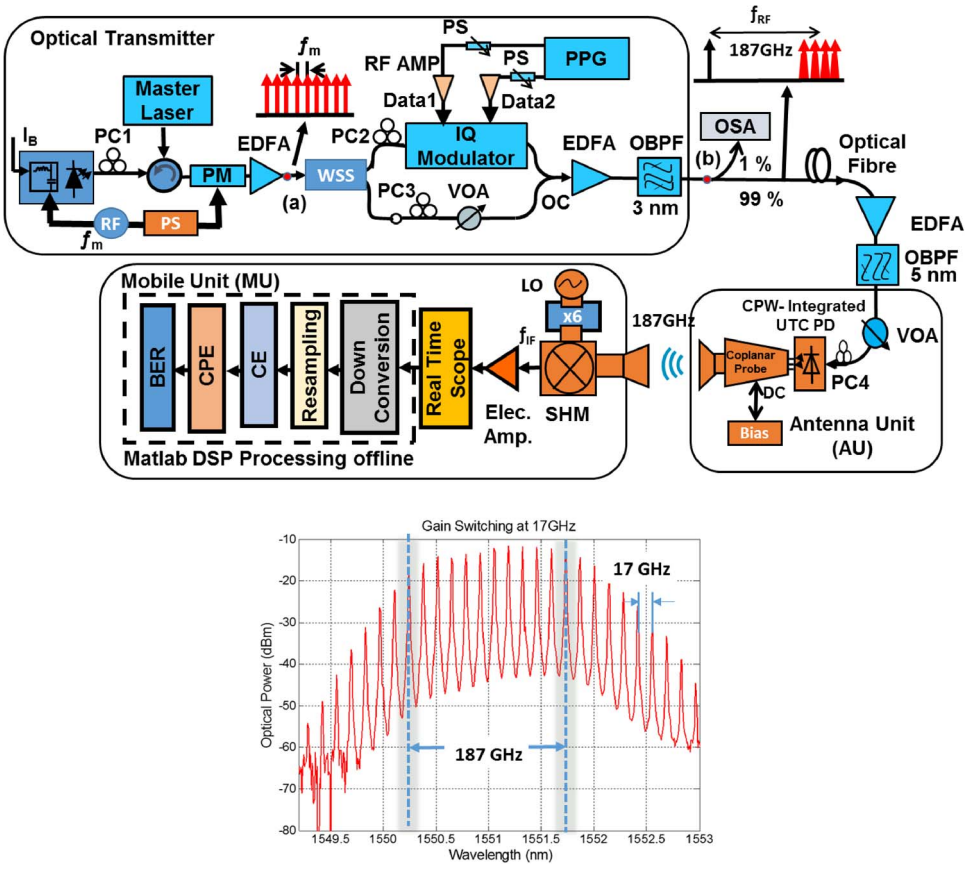

Fig. 2. Schematic diagram for multichannel THz signal experiment and the optical spectrum of the gain switched laser followed by the phase modulator at point (a).

the spectral efficiency to 2 bit/s/Hz using 12.5 GHz spaced optical carriers modulated with 12.5 GBaud QPSK signal.

2. Experimental Demonstration of a Single Carrier Wireless THz Signal Transmission Using Comb

The experimental arrangement used to demonstrate the photonic THz wireless-over-fiber (WoF) system, based on an externally injected gain-switched laser whose comb output was expanded with a phase modulator (PM) [8], is shown in Fig. 2. In the optical transmitter, a distributed feedback (DFB) laser at a wavelength of 1551 nm was used to generate a comb by gain switching the laser with the aid of a 24 dBm RF signal and DC bias applied via a bias tee. The spacing between the subcarriers was controlled by the driving RF frequency. The gain-switched laser was injection locked to a master laser with a linewidth of 300 kHz.

This process reduces the linewidth of each of the comb tones to that of the linewidth of the master laser [8]. The optical comb is then applied to the PM driven by an amplified sinusoidal waveform derived from the same signal generator used for gain-switching. A phase shifter (PS) was used to optimize the phase of the applied RF signal. Fig. 2 shows the spectrum of the comb at point (a) generated using the externally injected gain-switched laser followed by the phase modulator, with the comb line spacing set at 17 GHz. After amplifying the optical signal using an erbium-doped fiber amplifier (EDFA), a wavelength selective switch (WSS) was used to select two comb lines, spaced by 187 GHz (the desired THz frequency), into two different output ports. One of the optical tones was fed into an IQ Mach–Zehnder modulator (MZM) and modulated with QPSK modulation format. The I and Q signals driving the MZM were $2^{11} - 1$ pseudo-random bit

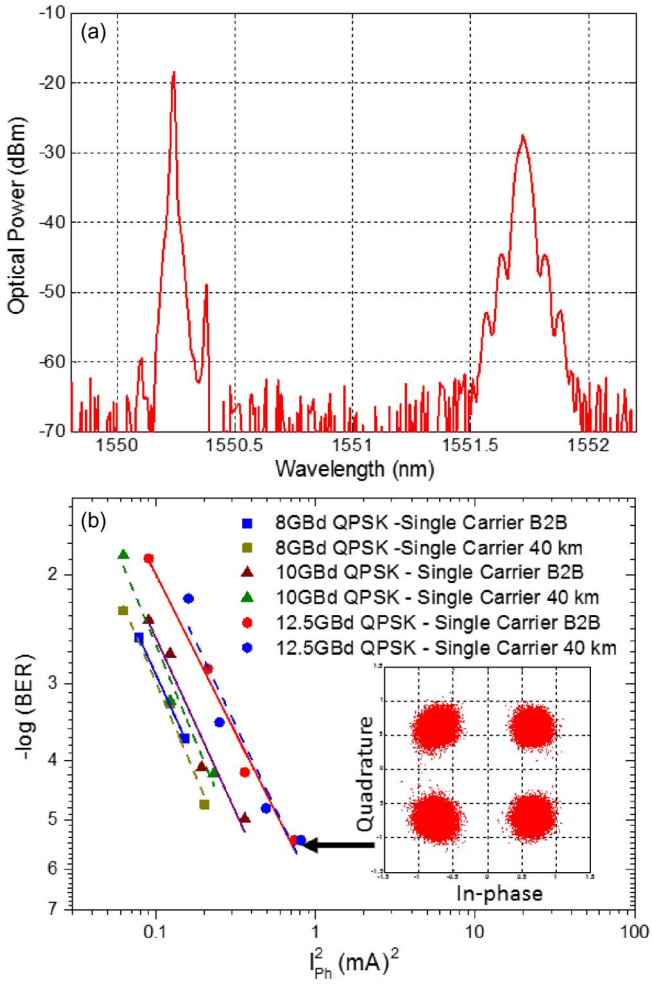

Fig. 3. (a) Optical spectrum for single carrier 8 Gbaud QPSK. (b) BER of a single carrier 8, 10, and 12.5 Gbaud QPSK versus photocurrent squared for B2B and after 40 km fiber. The inset is for the constellation diagram at lowest BER value.

sequence (PRBS) patterns obtained from independent outputs of a pulse pattern generator (PPG). The other optical tone was used as an optical local oscillator (LO) for THz signal generation by heterodyning with the modulated optical signal. The LO and modulated signals were combined in an optical coupler, aligning their polarizations by using a polarization controller (PC). The optical power of the LO was also controlled by a variable optical attenuator (VOA) to match the optical power of the modulated channel. The combined signal was then optically amplified and filtered using a 3 nm optical bandpass filter (OBPF) to remove out-of-band amplified spontaneous emission (ASE). A 99–1% optical coupler was used to capture the optical spectrum on an optical spectrum analyzer (OSA). The optical spectrum of the combined signal consisting of the modulated optical signal (8 Gbaud QPSK) and the LO is shown in Fig. 3(a). The delay between the two path lengths was accurately compensated in order to reduce the phase noise impact due to the phase decorrelation between the unmodulated and modulated signals [9]. The combined optical signal was transmitted over SSMF to the AU. An optical amplifier and VOA were used before the AU to evaluate the system performance. At the AU, the optical LO source beats with the modulated optical signal on an unpackaged uni-travelling carrier (UTC) photodiode with an integrated coplanar waveguide (CPW) output to generate the THz modulated multichannel signal. The output of the photodiode was coupled to a 20 dBi horn antenna (WR-5.1) using a coplanar millimeter-wave probe. The modulated THz signal was then radiated from the 20 dBi horn

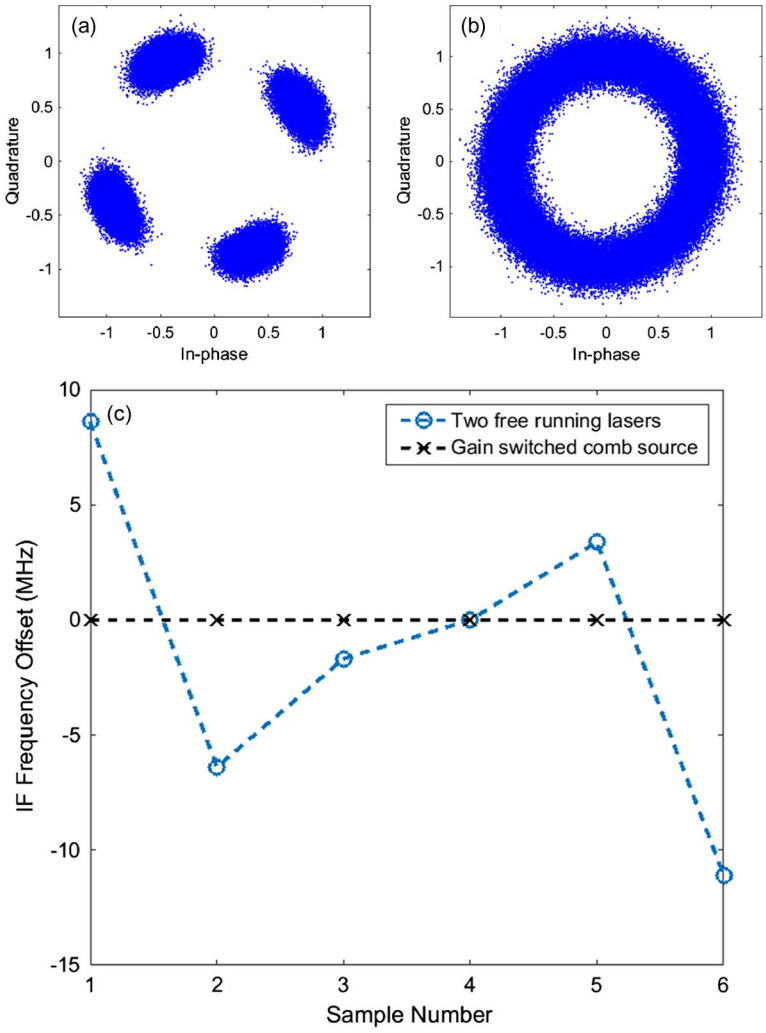

Fig. 4. Constellation diagrams for 10 Gbaud QPSK signal generated from (a) gain switched comb source and (b) two free running lasers and (c) IF frequency offset for different sampled data.

antenna and propagated over a 2 cm wireless channel to a receiving 20 dBi horn antenna. The received THz signal was initially down-converted to a microwave intermediate frequency (IF) by using a sub-harmonic mixer (SHM) operated with an electrical LO. The electrical LO source was obtained using a x6 electronic multiplier. The SHM mixes the second harmonic of the electrical LO with the received THz signal. The frequency of the RF signal generator was adjusted to place the IF signal at 23 GHz, within the frequency band of the analog-to-digital converter (ADC) in the real time scope (RTS). The received IF signal was then amplified and captured by the RTS whose sampling rate and bandwidth were 80 GSample/s and 36 GHz, respectively. The digitized signal was processed offline using the DSP blocks shown in Fig. 2 and explained previously in [5], although it should be noted that when using the gain-switched laser comb source frequency offset estimation (FOE) was not required. This was because the IF was accurately defined by the frequencies of the RF synthesisers used to drive the comb and the SHM. Thus the first step of the DSP step of digital downconversion to the baseband could be done using the nominal value of the IF, with very small residual frequency offset, as described later. The digitized IQ baseband signals were demodulated in subsequent steps of signal resampling, channel equalization (CE) based on blind equalization using the constant modulus algorithm (CMA), and carrier phase estimation (CPE) based on the fourth power Viterbi–Viterbi algorithm. After elimination of the $\pi/2$

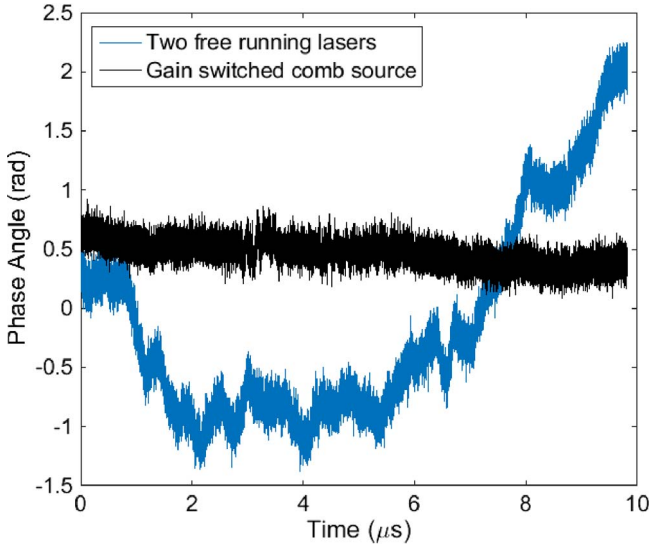

Fig. 5. Phase angle variations for the generated THz signal for two free running lasers and gain switched comb source.

phase ambiguity, the bit error ratio (BER) was calculated by directly counting the number of errors in the received bit stream.

To highlight the improvement in THz frequency stability with the comb source, Fig. 4(a) and (b) shows constellation diagrams after channel equalisation, but without frequency offset correction, for a 10 Gbaud QPSK signal when the THz signal is generated using the gain-switched laser comb source or two free-running lasers [5], respectively. In Fig. 4(a), the four constellation points are distinct and clearly separated of the gain switched comb source, whereas in Fig. 4(b) they are rotated to form an annulus due to the instability in the THz frequency generated using the two free running lasers. Fig. 4(c) shows the error from the nominal IF obtained by applying the FOE algorithm used in [5] to several different sets of data. With free-running lasers the IF was found to differ by up to 10 MHz from the nominal value from run to run, while when the gain-switched laser was used, a stable offset of around 13 kHz was obtained. This small offset could be due to calibration differences between the two synthesisers, which are increased by the comb generation and electrical LO multiplication processes.

The phase error that must be tracked was also reduced by using the gain-switched laser comb source instead of free-running lasers, as shown in Fig. 5, where the phase error estimated from the CPE block of the offline DSP (after frequency offset correction) is plotted for sample data sets for each case. With the comb source, the phase variation over the 10 μs long sample was small (with a variance σ^2 of 0.03 rad^2) compared to that for the case where the THz signal was generated using two free-running lasers ($\sigma^2 = 0.76$ rad^2). This is because the phase error of the signal generated using the comb source is largely determined by the multiplied phase noise of the RF synthesiser used to drive the gain-switched laser [10], whereas when free-running lasers are used the phase noise is dominated by the linewidths of the two lasers. These results show that using the gain-switched laser comb source instead of free-running lasers gives significant improvement in the accuracy with which the THz carrier frequency, and, thus, the IF, can be defined. This is particularly important when using multiple, closely spaced sub-carriers. Since both the frequency offset and the phase error variation are reduced by using the comb source, it is also expected that the DSP algorithms could be simplified, for instance by eliminating the FOE block and lowering the update rate of the CPE, thereby reducing the power dissipation associated with the receiver DSP.

The BER performance for wireless transmission using the comb source to generate 8, 10, and 12.5 Gbaud single-carrier QPSK signals at 187 GHz is shown in Fig. 3(b). The BER is

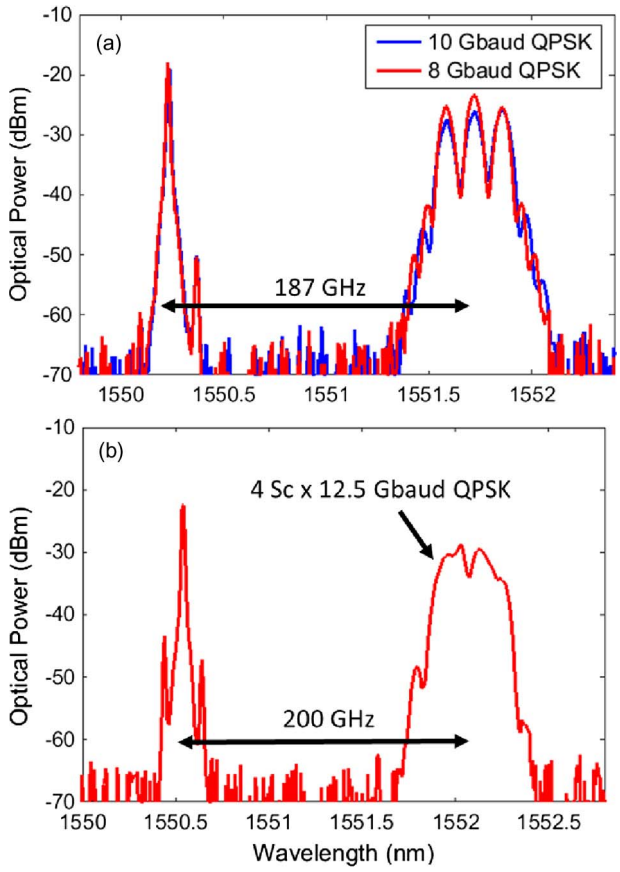

Fig. 6. Optical spectra for the multicarrier THz optical signal at point (b) in Fig. 2. (a) three subcarriers modulated with 8 Gbaud QPSK. (b) four subcarriers modulated with 10 Gbaud QPSK.

plotted against the square of the photocurrent, which is proportional to the received THz power for a fixed wireless link length. For each symbol rate, the BER was measured with the AU connected to the optical transmitter by a short length of optical fiber (B2B) and with the AU separated from the transmitter by 40 km of SSMF. Fig. 3(b) shows that the photocurrent squared (i.e., the received THz power) required to achieve a given BER (e.g., BER $= 10^{-3}$) increased as the symbol rate was increased, as would be expected. For all symbol rates, BERs as low as 10^{-5} were obtained, limited by the length of the data samples recorded on the RTS (around 1.25×10^5 symbols were used to estimate the BER), and no significant penalty was observed when fiber transmission was included. The inset in Fig. 3(b) shows the constellation diagram for B2B 12.5 Gbaud QPSK at the lowest BER value.

3. Experimental Demonstration Of Multichannel Wireless THz Signal Transmission

In the photonic multichannel THz WoF communication system, three or four optical subcarriers from the comb source were selected, and then QPSK-modulated by the same data generated by a PPG at 8, 10, and 12.5 Gbaud, as illustrated in Fig. 2. It has to be noted that the experiment was performed with correlated data on each subcarrier due to the limited lab resources, however, we have modeled the impact of the decorrelated data, as described in the next section. Two subcarrier spacings were investigated by controlling the driving RF frequency of the gain switched laser. For 8 and 10 Gbaud QPSK, three optical subcarriers spaced by 17 GHz were modulated with 8 or 10 Gbaud QPSK, giving a total wireless data rate of 48 or 60 Gb/s,

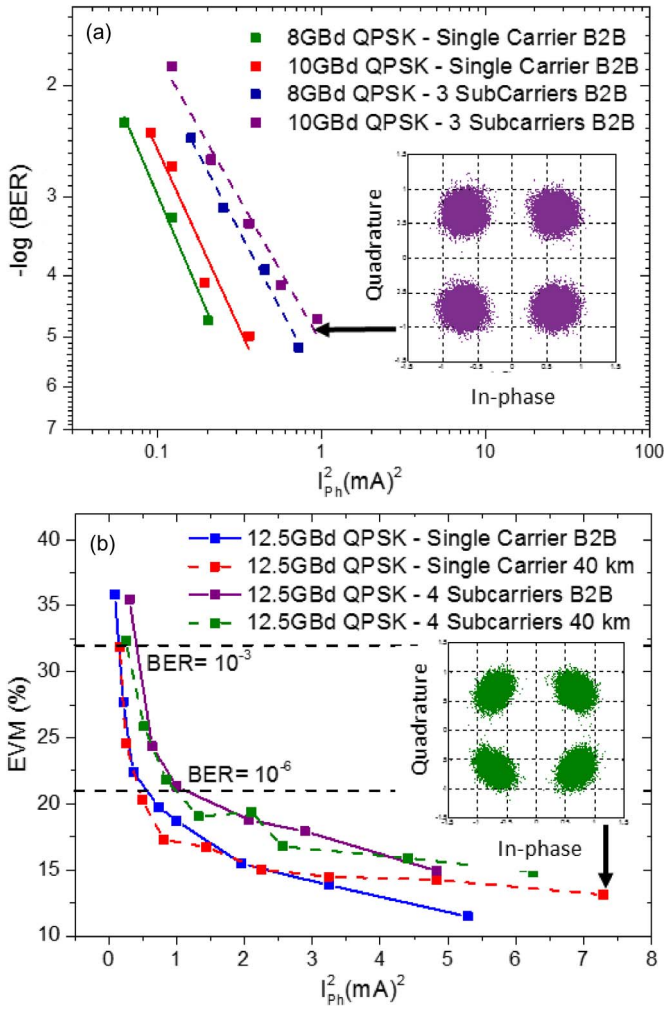

Fig. 7. (a) BER versus photocurrent squared for single and three subcarriers with 8 or 10 Gbaud QPSK. (b) EVM versus photocurrent squared for four subcarriers 12.5 Gbaud QPSK signal. The insets are the constellation diagrams at lowest BER.

respectively, with a spectral efficiency of around 1 bit/s/Hz. For 12.5 Gbaud QPSK, four selected optical subcarriers spaced by 12.5 GHz (i.e., with the subcarriers spaced at the baud rate) were modulated to achieve 100 Gb/s (spectral efficiency approaching 2 bit/s/Hz). Fig. 6(a) and (b) shows the spectra for the modulated optical subcarriers for the three-channel 8 and 10 Gbaud QPSK signals with 17 GHz channel separation and 187 GHz frequency offset, and for the four-channel, 12.5 Gbaud per channel case with 200 GHz frequency offset. At the receiver, each sub-channel was separately downconverted from the IF by using a digital LO to generate IQ baseband signals. The performance of the multichannel THz system was characterized by measuring BER on the middle subcarrier for the three-carrier 8 and 10 Gbaud signals and error vector magnitude (EVM) on one of the middle two subcarriers for the four carrier 12.5 Gbaud case. Middle subcarriers were selected for measurements because they will suffer the maximum interference from multiple adjacent subcarriers.

Fig. 7(a) shows the measured BER plotted against photocurrent squared (which is proportional to received THz power) for single- and three-subcarrier transmission with 8 and 10 Gbaud QPSK per subcarrier using the optical comb with line spacing of 17 GHz. All plots have a similar slope with no sign of an error floor at the lowest BER of around 10^{-5}, which is limited by the length of the data samples. When three subcarriers are transmitted, the power of each

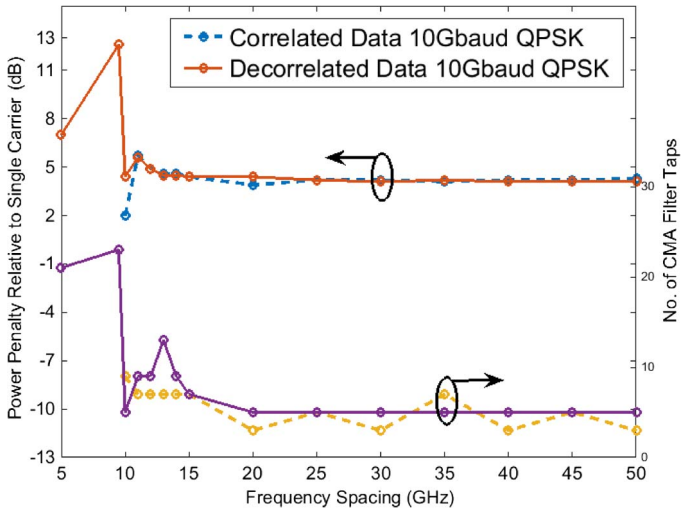

Fig. 8. Optical power penalty and number of CMA filter taps for different spacing at 10 Gbaud QPSK. (The dashed line is the simulation for the correlated data, and the dotted line is for the decorrelated data.)

subcarrier is approximately one third of that in the single subcarrier, hence we expect the photocurrent squared (i.e., the received THz power) required to achieve a given BER to be increased by a factor of three when three subcarriers are transmitted. Considering the 8 Gbaud results at a BER of 10^{-3}, we see that this is approximately true, with the photocurrent squared increasing from 0.1 mA^2 for a single subcarrier to 0.25 mA^2 for three subcarriers. A similar increase is observed for the results for 10 Gbaud QPSK per subcarrier. From these observations, we conclude that there is no significant crosstalk between the neighboring RF subcarriers.

Fig. 7(b) shows the experimental EVM results for one of the middle subcarriers for the case of 12.5 GBaud QPSK modulation on four subcarriers with 12.5 GHz spacing, compared to equivalent measurements for a single subcarrier. A relatively small increase in the photocurrent squared required for a given EVM was observed with four subcarriers (about a factor of two) at BER of 10^{-3}. Transmission over 40 km of fiber was found to have little effect on the performance. Although, in general, the penalty would be expected to increase when the channel spacing is reduced as a result of crosstalk when the adjacent channels overlap, the penalty is minimised by operating with a channel spacing equal to the baud rate and thanks to the phase correlation of the channels achieved by using the optical comb source [11]–[13]. Nonetheless, the observed penalty for four subcarriers compared to the single subcarrier case is less than the factor of four that would be expected due to the reduction of power per subcarrier. This is attributed to the data on the subcarriers being correlated in these experiments, as investigated further in the following section.

4. Simulation

In order to study the effect of the crosstalk between neighboring subcarriers, the system was simulated for three phase-correlated optical subcarriers with 10 kHz linewidth at different frequency spacings. The optical carriers were modulated simultaneously with the same data sequence (correlated), or with a different sequence for the middle channel (decorrelated data), using 10 Gbaud QPSK. Noise was added to change the optical signal-to-noise ratio before the PD. The THz signal after the PD was downconverted to IF (20 GHz) and then processed with the same DSP algorithm used in the experiment. Fig. 8 shows the optical power penalty of the middle channel relative to the single optical carrier at BER of 10^{-3} versus the frequency spacing between subcarriers for correlated and decorrelated data. There is no penalty difference between correlated and decorrelated data in the frequency range 15–50 GHz. The optical power in

each subcarrier is one third that of the single channel which results in a power penalty of about 4.8 dB (i.e., $10 * \log(3)$). When the channel spacing was reduced below 15 GHz and the signals start to overlap, the power penalty increases due to linear cross talk, as expected. However, when the frequency spacing is the same as the baud rate, a reduction in penalty is obtained due to phase correlation of the optical carriers [14], [15]. With correlated data, the penalty is reduced to approximately 2 dB, significantly less than the 4.8 dB penalty due to the reduction of power per channel. Below 10 GHz, it was not possible to demodulate the data and obtain BER $< 10^{-3}$, except at two points in the decorrelated case. The CMA filter length used in the simulation was optimized for each channel spacing. As shown in Fig. 8, the optimum number of CMA taps increased as the subcarrier spacing decreased. Slight differences were observed between the number of taps required for correlated and decorrelated data.

From these simulation results, we see that when the channel spacing is larger than the symbol rate there is almost no difference between correlated and decorrelated data, with the penalty observed being essentially that due to the reduction in power per channel. The experimental results for 8 or 10 Gbaud at 17 GHz channel spacing show a penalty of approximately 4.5 dB at a BER of 10^{-3} (from the ratio of the squared photocurrents for single and three subcarriers), in good agreement with simulation. We therefore conclude that the use of correlated data in our experiments allows the performance of a real system, with fully decorrelated data, to be adequately estimated under these conditions.

When the channel spacing is equal to the symbol rate, the experimental results at 12.5 Gbaud show a power penalty relative to the single channel case of approximately 4 dB (corresponding to the ratio of the squared photocurrents 0.15 and 0.35 mA^2 at BER of 10^{-3} for single and four subcarriers case), significantly lower than the $(10 * \log(4) = 6$ dB$)$ penalty associated with the reduction in power per channel for four subcarriers. This reduction in penalty with correlated data when the subcarrier spacing is equal to the baud rate is similar to what was obtained in the simulation. We thus conclude that the use of correlated data in the experiment can lead to an underestimate of the penalty under these conditions, with simulations suggesting that the penalty with decorrelated data in channels spaced at the baud rate would be similar to that due to the reduction in power per channel.

5. Conclusion

In conclusion, we have successfully demonstrated photonic generation of single and multichannel THz wireless signals at transmission rates up to 100 Gb/s at around 200 GHz carrier frequency using an externally injected gain-switched laser comb source. The demonstrated system generates a stable THz carrier frequency, with frequency and phase noise determined by the RF source used to drive the comb source. The improved frequency stability and phase noise performance compared to using free-running lasers is expected to allow the use of simplified DSP algorithms at the receiver, reducing power dissipation and processing delay. System evaluations were carried out for single and multicarrier THz wireless signals at 8, 10, and 12.5 GBaud, with and without 40 km fiber transmission between the optical transmitter and the remote antenna unit. The results obtained suggest that multicarrier transmission will allow transmission rates for high-speed THz wireless data applications to be increased at high spectral efficiency, while relaxing the bandwidth requirements for the optoelectronic components.

References

[1] A. Seeds, H. Shams, M. Fice, and C. Renaud, "TeraHertz photonics for wireless communications," *J. Lightw. Technol.*, vol. 33, no. 3, pp. 579–587, Feb. 2015. [Online]. Available: http://ieeexplore.ieee.org/lpdocs/epic03/wrapper.htm?arnumber=6892933

[2] X. Pang *et al.*, "100 Gbit/s hybrid optical fiber–wireless link in the W-band (75–110 GHz)," *Opt. Exp.*, vol. 19, no. 25, pp. 24 944–24 949, Dec. 2011. [Online]. Available: http://www.ncbi.nlm.nih.gov/pubmed/22273887

[3] J. Zhang *et al.*, "Multichannel 120-Gb/s data transmission Over 2 × 2 MIMO fiber–wireless link at W-band," *IEEE Photon. Technol. Lett.*, vol. 25, no. 8, pp. 780–783, Apr. 2013.

[4] S. Koenig *et al.*, "Wireless sub-THz communication system with high data rate," *Nat. Photon.*, vol. 7, no. 12, pp. 977–981, Oct. 2013.
[5] H. Shams *et al.*, "Photonic generation for multichannel THz wireless communication," *Opt. Exp.*, vol. 22, no. 19, pp. 23 465–23 472, Sep. 2014.
[6] A. Kanno, P. T. Dat, T. Kuri, I. Hosako, and T. Kawanishi, "Evaluation of frequency fluctuation in fiber–wireless link with direct IQ down-converter," in *Proc. ECOC*, 2014, pp. 6–8.
[7] P. M. Anandarajah *et al.*, "Generation of coherent multicarrier signals by gain switching of discrete mode lasers," *IEEE Photon. J.*, vol. 3, no. 1, pp. 112–122, Feb. 2011.
[8] R. Zhou *et al.*, "40 nm wavelength tunable gain-switched optical comb source," *Opt. Exp.*, vol. 19, no. 26, pp. B415–20, Dec. 2011.
[9] H. Takahashi, K. Okamoto, and T. Nagatsuma, "Low-phase noise photonic millimeter-wave generator using an AWG integrated with a 3-dB combiner," in *Proc. IEEE Topical Meet. MWP*, 2004, vol. 2, pp. 3–6.
[10] T. Shao, H. Shams, P. M. Anandarajah, M. J. Fice, C. C. Renaud, F. van Dijk, A. J. Seeds, and L. P. Barry, "Phase noise investigation of multicarrier THz wireless transmission system based on an injection-locked gain-switched laser," *IEEE Trans. Terahertz Sci. Technol.*, 2015. [Online]. Available: http://ieeexplore.ieee.org/stamp/stamp.jsp?tp=&arnumber=7101306&isnumber=5741778
[11] S. Chandrasekhar and X. Liu, "Experimental investigation on the performance of closely spaced multi-carrier PDM-QPSK with digital coherent detection," *Opt. Exp.*, vol. 17, no. 24, pp. 21 350–21 361, Nov. 2009.
[12] A. D. Ellis and F. C. G. Gunning, "Spectral density enhancement using coherent WDM," *IEEE Photon. Technol. Lett.*, vol. 17, no. 2, pp. 504–506, Feb. 2005.
[13] G. Goldfarb, G. Li, M. G. Taylor, and A. Optical, "Orthogonal wavelength-division multiplexing using coherent detection," *IEEE Photon. Technol. Lett.*, vol. 19, no. 24, pp. 2015–2017, Dec. 2007.
[14] W. Shieh, X. Yi, and Y. Tang, "Experimental demonstration of transmission of coherent optical OFDM systems," in *Proc. Conf. OFC/NFOEC*, 2007, pp. 1–3.
[15] S. K. Ibrahim *et al.*, "Towards a practical implementation of coherent WDM: Analytical, numerical, and experimental studies," *IEEE Photon. J.*, vol. 2, no. 5, pp. 833–847, Oct. 2010.